Ionics (2019) 25:1633–1643
https://doi.org/10.1007/s11581-018-2752-7

ORIGINAL PAPER

New oligoether plasticizers for poly(ethylene oxide)-based solid polymer electrolytes

Qiang Ma[1] · Amartya Chakrabarti[2] · Xinyi Mei[1] · Zheng Yue[1] · Hamza Dunya[1] · Robert Filler[1] · Braja K. Mandal[1]

Received: 1 August 2018 / Revised: 24 September 2018 / Accepted: 3 October 2018 / Published online: 5 November 2018

Abstract

Two new plasticizers, nitrile groups terminated oligoether (NOE) and lithium sulfonamide groups containing oligoether (LSA), have been synthesized to construct superior poly(ethylene oxide) (PEO)-based solid polymer electrolytes (SPEs). The chemical structures of these plasticizers were confirmed by FTIR, ^{1}H-NMR, and elemental analysis. The electrochemical and thermal properties of the resulting SPEs have been thoroughly evaluated. The SPEs containing varied weight ratios of these plasticizers along with different Li/O mole ratios of lithium bis(trifluoromethylsulfonyl)imide (LiTFSI) have been investigated to optimize the electrolyte systems. Both plasticizers displayed good ionic conductivity at elevated temperatures. The SPE containing 40 wt.% of NOE in 12:1 PEO-LiTFSI complex showed ionic conductivity of 1.11×10^{-4} S cm^{-1} at 312 K, while the SPE containing 10 wt.% of LSA in 12:1 PEO-LiTFSI complex showed 5.08×10^{-5} S cm^{-1} and 1.88×10^{-4} S cm^{-1} at room temperature and 312 K, respectively. Most notably, the SPE containing 10 wt.% LSA in 14:1 PEO-LiTFSI complex displayed ionic conductivity of 1.01×10^{-3} S cm^{-1} at 343 K. Moreover, these SPEs exhibited good electrochemical stability (~4.2 V vs. Li^{+}/Li) and displayed no noticeable thermal degradations below 350 °C.

Keywords Lithium-ion batteries · Solid polymer electrolytes · Oligoether plasticizers · Ionic conductivity · Electrochemical stability

Introduction

In the past decade, the development of solid polymer electrolytes (SPEs) has drawn immense attention for application in lithium-ion (Li-ion) batteries, because of their several advantages over liquid electrolytes [1–5]. In the absence of traditional organic electrolytic solvents, such as ethylene carbonate (EC) and dimethyl carbonate (DMC), SPEs eliminate hazards of fire and environmental pollution and increase the efficacy of manufacturing large flat type devices [6–8]. Potential problems associated with the leakage of harmful liquid electrolytes can also be avoided by using SPEs. Among the solvent-free polymer electrolyte systems, polyethylene oxide (PEO) is most commonly used because of its chemical, mechanical, and electrochemical stabilities [9–12]. PEO contains only strong and unstrained C–O, C–C, and C–H bonds. The repeat unit, –CH_2CH_2O–, provides ideal spacing to solvate a maximum number of lithium ions. Also PEO contains a Lewis base, dioxyethylene group, to facilitate the dissolution of lithium salts due to facile chelation with the cations. Despite these positive features of PEO-based SPEs, they exhibit very poor ambient temperature ionic conductivity (< 10^{-5} S cm^{-1}), due to very high degree of crystallinity present in PEO at room temperature [13, 14]. Ion conduction in an SPE is believed to occur smoothly in the amorphous region, because of greater segmental mobility of the amorphous phase [15].

Several effective strategies have been reported to improve the ionic conductivity of PEO-based electrolytes by increasing amorphous content of the SPEs [16–20]. For example, the presence of undesired crystalline domains in PEO electrolytes can be substantially eliminated by blending with inert ceramic nano-sized particles (viz., Al_2O_3, SiO_2, and TiO_2) which are believed to kinetically inhibit crystallization of the amorphous phase [21–24]. Both low and high molecular weight liquid

✉ Braja K. Mandal
mandal@iit.edu

[1] Department of Chemistry, Illinois Institute of Technology, Chicago, IL 60616, USA

[2] Department of Physical Sciences, Dominican University, River Forest, IL 60305, USA

plasticizers have been also studied to allow higher ionic mobility [25–28]. Besides, the dynamics of segmental motion of polymer complexes, ion hopping process is another important factor to affect ion conduction in polymer electrolytes [29]. Systematic studies have been reported on the effect of different salts and compositions in PEO-Li system [30, 31]. Doping of ionic liquids (ILs), consisting of bulky organic cation, such as EMIMTFSI and $BMIMPF_6$, have been reported to improve ionic conductivity due to higher delocalized charges, as well as enhancement of amorphous content [32–35].

A few years ago, we reported a star-shaped oligoether-based borate ester plasticizer to address the ionic conductivity issue of PEO-based SPEs [36]. The results demonstrated that such a material significantly improved ionic mobility, leading to the increment of ionic conductivity of PEO-based SPEs at room temperature. The borate ester–plasticized SPEs also exhibited excellent thermal and electrochemical stabilities. In this study, we present another two new oligoether-based plasticizers in which one (NOE) is terminated with nitrile groups and the other (LSA) contains lithium sulfonamide moieties. NOE is terminated with multiple polar nitrile groups to increase the dielectric constant of the matrix, which allows high degree of dissociation of lithium salts, leading to enhanced ionic conductivity of the polymer matrix. LSA contains lithium sulfonamide moieties, which provide additional charge carriers—another approach to increase ionic conductivity. The synthesis and preliminary electrochemical properties of these materials are presented in this article.

Materials and methods

Materials

Polyether diamine (Jeffamine ED®-600) and polyetheramine (Jeffamine M®-600) were obtained as a gift from Huntsman Corporation, Woodlands, TX, USA. Lithium bis(trifluoromethylsulonyl) imide (LiTFSI) was also obtained as a gift from Minnesota Mining and Manufacturing Company (3M), Maplewood, MN, USA. Acrylonitrile, benzene 1,3-disulfonyl chloride, triethylamine, lithium methoxide, and poly(ethylene glycol) dimethyl ether (OEG, $M_n \sim 1000$) were all purchased from Sigma-Aldrich Company and used as received without further purification. All organic solvents were purchased from Fisher Scientific Company.

NMR and elemental analysis

^{1}H NMR spectra (300 MHz Bruker NMR Spectrometer) and elemental analysis (Perkin Elmer 2400 CHNS Elemental Analyzer) were used to confirm the structures and purity of the products.

Synthesis of NOE

5.032 g (8.387 mmol) of ED-600, 8.098 g (152.79 mmol) of acrylonitrile, and 5.0 mL of deionized water were taken in a 50-mL single-neck flask fitted with a reflux condenser. The resulting solution was stirred for 0.5 h at room temperature, followed by heating at 100 °C for 24 h. After completion, the reaction mixture was cooled to ambient temperature and extracted with 30 mL of dichloromethane (DCM). The organic layer was dried over anhydrous sodium sulfate to give a highly viscous colorless product after removal of the solvent under high vacuum (Scheme 1). Yield: 6.7 g (98%). FTIR (neat): 2868, 2246, 1419, 1109, 686 cm^{-1}. ^{1}H-NMR (300 MHz, $CDCl_3$): δ 2.45–2.53 (q). Elemental analysis: Calcd. for $C_{41}H_{74}O_{11}N_6$: C, 59.54; H, 9.02; N, 10.16. Found: C, 59.42; H, 8.88; N, 10.01.

Synthesis of LSA

Di-sulfonamide intermediate

0.9062 g benzene 1,3-disulfonyl chloride (1.0 eq.) and 4.2376 g of M-600 (2.1 eq.) were placed in a 50-mL three-neck flask containing 15 mL of DCM. The flask was put in an ice water bath. 1.0729 g triethylamine (3.0 eq.) was dissolved in 10 mL DCM, and the solution was added dropwise to the flask. The whole mixture was stirred under argon protection. After overnight reaction, the mixture was filtered through cotton and rotovap the solvent. Ten milliliters ether was added to the flask, and the ether solution was filtered through cotton and again rotovap the solvent. Fifteen milliliters hexane was added to the flask, and the solution was kept in the freezer for 3 h then decanted the top layer. The process was repeated three times to remove any unreacted hexane soluble M-600. The product was concentrated and dried in vacuo. Yield: 3.75 g (81%). FTIR (neat): 2971.7, 1582.8, 1107.8 cm^{-1}. ^{1}H-NMR (300 MHz, $CDCl_3$): δ 8.38 (s), 8.15 (d), 7.60 (t), 6.22 (s), 5.95 (s). Elemental analysis: Calcd. for $C_{66}H_{128}O_{24}N_2S_2$: C, 56.71; H, 9.23; N, 2.00; S, 4.59. Found: C, 56.66; H, 9.11; N, 1.88; S, 4.56.

Lithiation of di-sulfonamide intermediate (LSA)

0.2135 g lithium methoxide (2.1 eq.) and 3.7459 g sulfonamide (1.0 eq.) were dissolved in 30 mL anhydrous methanol. The mixture was stirred for 4 h at room temperature. After the reaction methanol was removed in a rotavap and 30 mL anhydrous THF was added to the flask. The solution was filtered through cotton, concentrated, and dried in vacuo. Scheme 2 depicts the synthetic route to LSA. Yield: 3.83 g (98%). FTIR (neat): 2971.4, 1582.4, 1108.7 cm^{-1}. ^{1}H-NMR (300 MHz, $CDCl_3$): δ 8.38 (s), 8.15 (d), 7.60 (t). Elemental analysis:

Scheme 1 Synthesis of NOE, a nitrile group-terminated OEG plasticizer

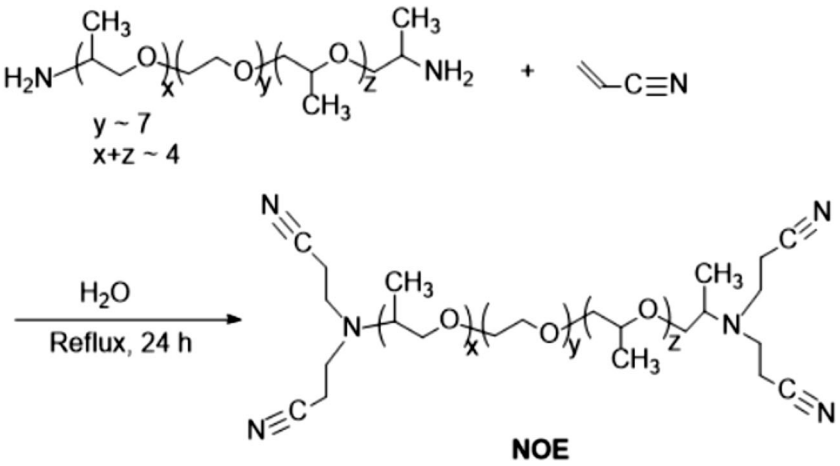

Calcd. for $C_{66}H_{126}O_{24}N_2S_2Li_2$: C, 56.23; H, 9.01; N, 1.99; S, 4.55. Found: C, 56.21; H, 9.04; N, 1.92; S, 4.42.

Preparation of SPE films

PEO (M_v ~ 5,000,000) was chosen as the polymer for the base matrix, and LiTFSI was used as the primary source of lithium ions. All PEO-LiTFSI complexes with various compositions were prepared by dissolving the components in anhydrous acetonitrile in a glove box, poured in a petri dish followed by drying under high vacuum at 60 °C overnight. The resulting thin film was peeled off from the petri dish, folded, and placed in between two Teflon-coated sheets to prepare thin film SPEs. The whole sandwich assembly was then hot pressed in a Carver press at 150 °C with a pressure of about 15,000 psi. Two rectangular stainless-steel plates of desired dimension were used as a spacer in order to obtain the desired thickness (~ 0.150 mm) of the film. Once the film was made, it was rapidly transferred into a glove box to assemble the set-up for cyclic voltammetry and other electrochemical measurements. Minimum exposure of the films to the environment was allowed to reduce the moisture absorption by the highly hygroscopic lithium salts that are incorporated into the films.

Formulations of NOE-plasticized SPEs

The weight percentage of NOE in the polymer matrix was varied from 10 to 40 wt.% to produce four different polymer films (Table 1). The amount of plasticizer incorporated into the polymer matrix was optimized by observing the free-standing nature of O/Li = 12:1 PEO-LiTFSI complexes containing 1.0 g of PEO and 0.5437 g LiTFSI.

Formulations of LSA-plasticized SPEs

First, SPE sample films of different compositions of LSA from 0.1 to 0.3 g were prepared in the ratio of O/Li = 12:1 PEO-LiTFSI complex (shown in Table 2). Second, 0.1 g LSA was taken to mix with different ratios of PEO-LiTFSI complex from 10:1 to 16:1. Finally, 0.1 g OEG was used to compare with 0.1 g LSA plasticizer in different PEO-LiTFSI complexes (Table 3).

Glass transition temperature (T_g) measurement

Differential scanning calorimetry (DSC) measurements of SPEs films were conducted to explain the decrease in crystallinity of the polymer complex when the additive was added. DSC data were obtained between − 100 and 150 °C using a Mettler differential scanning calorimeter. Two segments of DSC scanning included the following: (1) − 100 °C isothermal for 10.0 min with Argon purge at 70.0 mL/min, (2) − 100 to 150 °C with a heating rate at 10 °C/min under Argon purge at 70.0 mL/min. An empty aluminum pan was used as a reference.

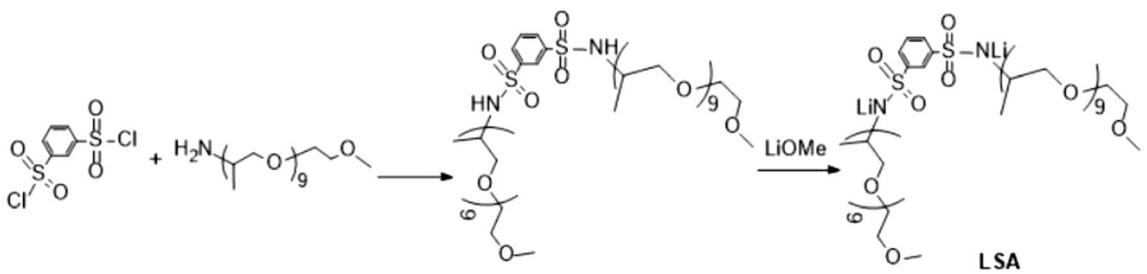

Scheme 2 Synthesis of LSA, an OEG plasticizer containing two lithium sulfonamide moieties

Table 1 Formulation of varied amounts of NOE in 1.0 g 12:1 PEO-LiTFSI complex

Sample	SPE0	NOE-12a	NOE-12b	NOE-12c	NOE-12d
NOE (g)	–	0.1	0.2	0.3	0.4

Measurement of ionic conductivity at different temperatures

Ionic conductivities of all films were determined from room temperature to 70 °C by means of complex impedance measurements using a computer-controlled Solartron impedance analyzer (model-1260) over the frequency range of 100 to 0.1 Hz. The detailed version of the procedure was published by our group earlier [36]. The bulk resistance was obtained from the high-frequency intercept of the real axis from the complex impedance plot. The conductivity was calculated using the following equation:

$$\sigma = l/\mathrm{RbA}$$

In this equation, l is the thickness and A is the area of the respective films. R_b is the measured bulk resistance. The samples were sandwiched between two stainless-steel blocking electrodes and placed in a temperature-controlled oven.

Electrochemical and thermal stability measurements

The electrochemical window of all plasticized SPEs was obtained by the cyclic voltammetric method using a Solartron impedance analyzer (model-1260). A test cell was assembled to determine the oxidation potential at room temperature with stainless steel as working electrode and lithium foil serving as the counter and reference electrode. For NOE plasticizers, the potential was anodically scanned from 2.0 to maximum 5.0 V versus Li/Li^+ at a scan rate of 10 mV/s.

The thermal stability of SPE films has been tested by Mettler thermogravimetric analyzer (TGA). Five segments of TGA scanning included the following: (1) 25~110 °C heating at 10.0 °C/min with Argon purge at 70 mL/min, (2) 110 °C isothermal for 10.0 min with Argon purge at 70 mL/min, (3) 110~25 °C cooling at 10.0 °C/min with Argon purge at 70 mL/min, (4) 25 °C isothermal for 15.0 min with Argon purge at 70 mL/min, (5) 25~550 °C heating at 10.0 °C/min with Argon purge at 70 mL/min.

Table 2 Formulation of varied amounts of LSA in 1.0 g 12:1 PEO-LiTFSI complex

Sample	SPE0	LSA-12a	LSA-12b	LSA-12c
LSA (g)	–	0.1	0.2	0.3

Table 3 Formulations of 10 wt.% (0.1 g) of LSA and OEG plasticizers in varied ratios of PEO-LiTFSI complex

Ratio of O/Li	10:1	12:1	14:1	16:1
Sample with 10 wt.% of LSA	LSA-10a	LSA-12a	LSA-14a	LSA-16a
Sample with 10 wt.% of OEG	OEG-10a	OEG-12a	OEG-14a	OEG-16a

Results and discussion

Structural characterization

Structure analysis of the NOE plasticizer

The NOE was synthesized in one step by the Michael addition reaction between a commercially available amine-terminated oligoether (ED-600) and acrylonitrile in almost quantitative yield (Scheme 1). The product was characterized by FTIR (neat) and ^{1}H-NMR (300 MHz, $CDCl_3$). The IR absorption peak at 2246 cm^{-1} was attributed to the nitrile group stretching frequency, which is slightly more (2230 cm^{-1}) than that of the nitrile group displayed for acrylonitrile. The lower wave number for acrylonitrile is due to the resonance between the double bond and the carbonyl group. No absorption peaks in between 3000 to 3100 cm^{-1} (sp^2 carbon-hydrogen stretching) indicated the absence of trace acrylonitrile presented in the product. The only signal, δ 2.45–2.53 (q), present in the ^{1}H-NMR also supported the proposed structure of the plasticizer. No vinyl proton peaks around 6 ppm corresponding to the hydrogens in acrylonitrile were not observed. NOE is readily soluble in common organic solvents and miscible in PEO.

Structure analysis of the LSA plasticizer

LSA was synthesized in two steps by connecting oligoether segments (M-600) around benzene sulfonamide moieties followed by lithiation on the nitrogen atom of the sulfonamide group (Scheme 2). The product was characterized by FTIR (neat) and ^{1}H-NMR (300 MHz, $CDCl_3$). The IR absorption peaks at 2971.4 cm^{-1} and 1582.8 cm^{-1} are attributed to alkyl C–H and sulfonamide N–S stretching frequencies, respectively. The shift of sulfonyl group shifted from 1410 to 1370 and 1204–1166 cm^{-1} to 1330–1290 and 1130–1100 cm^{-1}, respectively, indicating the successful reaction between amine and sulfonyl chloride to sulfonamide. The peaks in the ^{1}H-NMR also supported the structure of the benzene sulfonamide compound: disappearance of signals of M-600 at 3.12 (m) and appearance of 6.22 (s), 5.95 (s) after the first-step reaction with

benzene disulfonyl chloride. Peaks at 6.22 (s), 5.95 (s) were disappeared in the final-step confirming a successful lithiation process.

Ionic conductivity

Ionic conductivity study of NOE plasticizer

In the PEO system, the best ionic conductivity is observed when one molecule of lithium salt (e.g., LiTFSI) is present for about every 12 repeat units of ethylene oxide segment [36–38]. The effect of NOE content in PEO-based SPEs has been thoroughly investigated in this study. Different weight percentages (10 to 40) of the material have been added to O/Li = 12:1 PEO-LiTFSI complex to make homogeneous films. An electrolyte film without the NOE additive was also examined and served as the reference. Figure 1 depicts the temperature dependence of ionic conductivity with respect to the plasticizer content. It is apparent that the ionic conductivities of the films containing plasticizers have been markedly improved compared to the reference electrolyte. The ionic conductivity values have been summarized in Table 4. High ionic conductivity values (3.46×10^{-5} S cm^{-1} at 298 K, 5.00×10^{-5} S cm^{-1} at 303 K) were obtained for 10 wt.% of NOE in PEO-LiTFSI compared to recently published reports: 10 wt.% of TiO_2 and Al_2O_3 as nano-fillers in PEO-$LiCF_3SO_3$ systems displayed 4.9×10^{-5} S cm^{-1} at 303 K and 2.02×10^{-5} S cm^{-1} at 298 K, respectively, while PEO-LiTFSI-LGPS organic-inorganic hybrid composite electrolyte and organic plasticizer PEG in PEO-$LiCF_3SO_3$ systems showed 1.18×10^{-5} S cm^{-1} and 1.71×10^{-5} S cm^{-1} at 298 K, respectively. Even when we compare NOE with our previously published work on borate ester plasticizers [36], we could see that NOE plasticizer displayed remarkable improvement—10 times enhancement in ionic conductivity vs. 2.5 times enhancement for borate ester plasticizers. It is noteworthy that the SPE containing 40 wt.% of NOE showed the highest ionic conductivity (7.18×10^{-4} S cm^{-1} at 343 K). This result is attributed to the fact that the structure of NOE contains an oligoether segment terminated with nitrile groups. This molecular design has two key features that are expected to improve SPE properties: compatibility with the PEO host and superior ionic dissociation across the electrolyte film. The presence of oligoether moiety helps to prevent phase segregation of salt from the host film and reduce crystalline content of the PEO matrix [39]. The presence of polar nitrile groups in the film is also expected to increase the dielectric constant—a condition favors greater ionic dissociation, leading to higher ionic conductivity [31, 34]. However, NOE did not supply any ions to the electrolyte system. The only source of lithium cations was from dissolution of LiTFSI in PEO complex. The following section on the LSA plasticizer explains the effect of additional source of lithium cation from the plasticizer.

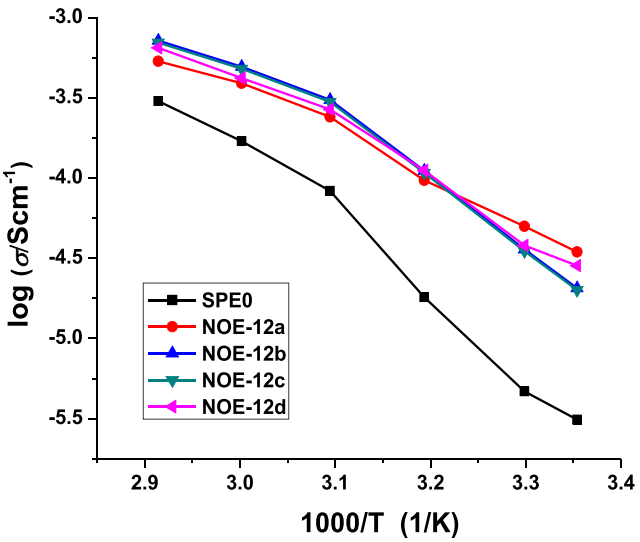

Fig. 1 Ionic conductivity versus temperature of NOE containing O/Li = 12/1 PEO-LiTFSI complexes

Ionic conductivity study of the LSA plasticizer

Similar to the NOE design, the presence of oligoether groups in LSA helps to improve the chain flexibility and polar sulfonamide groups increase dielectric constant of the polymer matrix. Both parameters have direct relationship with the ionic conductivity. However, in LSA, one equivalent of compound contains two equivalents of lithium ions and oligoether chains. Moreover, two chains are connected *meta* to each other on the aromatic ring, which can prevent crystallinity due to lack of symmetry. In addition, the negative charge on the nitrogen atom is delocalized by resonance with the adjacent sulfone group, making the lithium ion more mobile (low lattice energy)—a situation favors ionic conductivity.

In this study, we explored the effect of the amount of LSA in PEO-LiTFSI complex and the lithium salt concentration with a certain LSA content. OEG, as a standard additive, was also studied under varied amounts of lithium salt concentrations. Ionic conductivities of the weight percentages from 10 to 30 of LSA in 12:1 PEO-LiTFSI system and PEO-LiTFSI sample without any additive were measured. Figure 2a shows the dependence of the conductivity on $1/T$ for different contents of LSA in O/Li = 12:1 PEO-LiTFSI complex in the temperature range from 298 to 343 K. The ionic conductivity data are summarized in Table 5. It can be noticed that the ionic conductivity markedly increased with the addition of LSA; however, at higher loading, the conductivity begins to drop. As mentioned earlier, oligoether chains can help lithium ions to coordinate and transport. However, in our case, the material contains both oligoether chains and lithium ions. Therefore,

Table 4 Comparison of ionic conductivity: present work vs. recently reported work

Polymer electrolyte compositions	Ionic conductivity (S cm^{-1})	References
PEO-$LiCF_3SO_3$-10%TiO_2	4.9×10^{-5} (303 K)	[40]
PEO-LiTFSI-1%LGPS	1.18×10^{-5} (298 K)	[41]
PEO-$LiCF_3SO_3$-10%Al_2O_3	2.02×10^{-5} (298 K)	[42]
PEO- $LiCF_3SO_3$-15%PEG	1.71×10^{-5} (298 K)	
PEO-LiTFSI-NOE-12a	3.46×10^{-5} (298 K) 5.00×10^{-5} (303 K)	Present work

adding too much amount of plasticizer would reverse the behavior, which could explain the ionic conductivity of LSA-12b decreased slightly compared to LSA-12a, while that of LSA-12c dropped a lot. In this series of the plasticizer, LSA-12a displayed the highest ionic conductivity of 5.08×10^{-5} S cm^{-1} at 298 K.

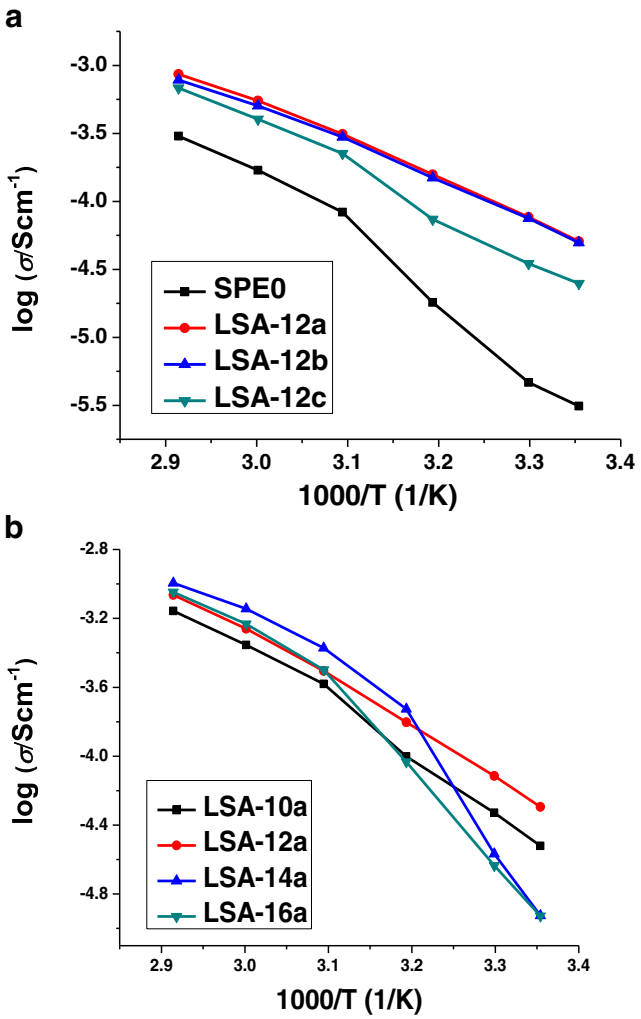

Fig. 2 Ionic conductivity versus temperature of different compositions of LSA in 12/1 PEO-LiTFSI complexes (**a**); 10 wt.% of LSA in different PEO-LiTFSI complexes (**b**)

Ionic conductivity of different compositions of lithium salt in the LSA-PEO-LiTFSI system has been thoroughly investigated in this study. Figure 2b depicts ionic conductivities of 10 wt.% of LSA in varied PEO-LiTFSI complexes from O/Li = 10:1 to 16:1. It is obvious to see that LSA-12a performed best at low temperature (298 K and 303 K), while LSA-14a exceeded at 313 K and displayed best conductivity at high temperature (1.88×10^{-4} S cm^{-1} at 313 K and 1.01×10^{-3} S cm^{-1} at 343 K). The data related to this study are summarized in Table 5. At low temperature (below 313 K), the vibrational segmental mobility is weak and lithium ions on LSA are not fully dissociated. Therefore, the polymer electrolytes with high concentrations of low lattice energy lithium salt performed better. By contrast, as the temperature increases (over 313 K), the dissociation energy for lithium ion is sufficient. Consequently, more free lithium ions drift in the system. However, once the dissociated lithium ions reach a certain value, the excess dissociated lithium ions may form ion pairs or ion clusters with counter anions, which reduces the free carriers' concentration and leads to the decrease in ionic conductivity. Moreover, the inter- and intra-molecular coordination between Li^+ and ethylene oxide (EO) units facilitates with the increase of lithium ions, leading to increase of T_g and decrease of ionic mobility [43, 44]. At this point, polymer electrolytes originally with lower lithium salt concentration would exhibit a better result, because as the temperature increases the dissociated lithium ions plus original lithium ions might just meet the proper value to reach the maximum ionic conductivity. In our case, O/Li = 14:1 PEO-LiTFSI was the right composition. By contrast, lower concentration like 16:1 could not provide enough free carriers in the electrolyte to achieve high ionic conductivity.

The effect of the structural design of LSA was further studied by comparing its properties with OEG, which is a low molecular weight (M_n ~ 1000) linear oligoether. Figure 3 illustrates comparisons of conductivities of 10 wt.% LSA and OEG in (a) 12:1and (b) 14:1 PEO-LiTFSI complexes. In Fig. 3a, the sample containing LSA exhibited slightly better conductivities than the sample containing OEG. On the other hand, the SPEs containing LSA and OEG in 14:1 PEO-LiTFSI complex displayed similar results at low temperatures (298 K and 313 K); however, at elevated temperatures, LSA-

Table 5 Ionic conductivity (S cm^{-1}) vs. temperature data for the proposed electrolytes

Temperature	298 K	303 K	313 K	323 K	333 K	343 K
Different compositions of NOE and LSA in 12:1 PEO-LiTFSI systems						
SPE0	3.12×10^{-6}	4.66×10^{-6}	1.80×10^{-5}	8.31×10^{-5}	1.69×10^{-4}	3.02×10^{-4}
NOE-12a	3.46×10^{-5}	5.00×10^{-5}	9.67×10^{-5}	2.41×10^{-4}	3.89×10^{-4}	5.35×10^{-4}
NOE-12b	2.84×10^{-5}	3.80×10^{-5}	1.11×10^{-4}	2.67×10^{-4}	4.19×10^{-4}	6.47×10^{-4}
NOE-12c	2.00×10^{-5}	3.49×10^{-5}	1.08×10^{-4}	2.98×10^{-4}	4.80×10^{-4}	6.98×10^{-4}
NOE-12d	2.06×10^{-5}	3.59×10^{-5}	1.11×10^{-4}	3.07×10^{-4}	4.93×10^{-4}	7.18×10^{-4}
LSA-12a	5.08×10^{-5}	7.68×10^{-5}	1.58×10^{-4}	3.12×10^{-4}	$5.49 \times 10–4$	8.62×10^{-4}
LSA-12b	4.96×10^{-5}	7.50×10^{-5}	1.49×10^{-4}	2.97×10^{-4}	$5.04 \times 10–4$	7.82×10^{-4}
LSA-12c	2.49×10^{-5}	3.48×10^{-5}	7.38×10^{-5}	2.25×10^{-4}	$4.03 \times 10–4$	6.83×10^{-4}
Different compositions of LiTFSI (O/Li = 10:1 to 16:1) in 10 wt.% LSA and PEO-LiTFSI systems						
LSA-10a	3.02×10^{-5}	4.70×10^{-5}	9.97×10^{-5}	2.63×10^{-4}	4.42×10^{-4}	6.97×10^{-4}
LSA-12a	5.08×10^{-5}	7.68×10^{-5}	1.58×10^{-4}	3.12×10^{-4}	5.49×10^{-4}	8.62×10^{-4}
LSA-14a	1.19×10^{-5}	2.71×10^{-5}	1.88×10^{-4}	4.24×10^{-4}	7.16×10^{-4}	1.01×10^{-3}
LSA-16a	1.18×10^{-5}	2.31×10^{-5}	9.28×10^{-5}	3.17×10^{-4}	5.86×10^{-4}	8.95×10^{-4}
Effect of 10 wt.% OEG (standard plasticizer) in PEO-LiTFSI systems						
OEG-12a	4.10×10^{-5}	6.00×10^{-5}	1.62×10^{-4}	2.74×10^{-4}	4.72×10^{-4}	6.89×10^{-4}
OEG-14a	1.29×10^{-5}	2.43×10^{-5}	7.55×10^{-5}	2.78×10^{-4}	4.59×10^{-4}	6.80×10^{-4}

contained sample showed improved conductivities compared with the SPE containing OEG. These superior results are presumably due to the presence of lithium ions in LSA. It is well known that the conductivity is directly proportional to mobility of ions and segmental motion of polymer chains [45]. In Fig. 3b, at low salt content system, the free lithium ions have not reached the peak point and lithium ions from LSA would increase the free carriers to favor ionic conductivity. By contrast, at high temperature, there is sufficient energy provided to dissociate more lithium ions, which explains why there is a gap between two curves at over 313 K. At slightly higher lithium salt concentrations, such as in Fig. 3a, LSA as the additive showed better conductivity results except at 313 K, because at this temperature, LSA dissociates more lithium ions to reduce the free carriers in the system due to ion pair and ion cluster formation, which reduces both ions' mobility and segmental motion. However, with increasing temperature, the chain flexibility increases to enhance ionic conductivity. The conductivity values of OEG (standard plasticizer) in PEO-LiTFSI complexes are given in Table 5.

DSC investigations of NOE and LSA

To better understand the behavior of lithium-ion transport under the influence of the NOE plasticizer, the thermal phase transition characteristics of the SPE films were tested by the DSC. The glass transition temperature, T_g, is a specific feature of a polymer's amorphous region. A flexible chain exhibits a low T_g, whereas a rigid chain shall have a high T_g value. A decrease in the value of T_g helps in the easy movement of the polymer chains, thus provides smooth transport of ions (i.e., increases ionic conductivity). Figure 4 shows the DSC curves for both the reference and a NOE-plasticized electrolyte (e.g., 12d). The addition of NOE to a PEO sample dramatically reduces the crystalline content in the sample. This is evident by the marked reduction of area under the crystalline phase melting region; however, only a slight reduction in T_g was observed for the plasticized samples. For example, SPE0 displayed a T_g of − 30.5 °C with the onset at − 37.3 °C, while NOE-12d showed the transition at − 33.0 °C with an onset at − 39.8 °C.

DSC investigation can help us to further understand the structural advantages of LSA over OEG. It is well established that an OEG additive can reduce the crystalline phase of PEO-based SPE system to increase the ionic conductivity [46–49]. A comparative measurement was studied between 10 wt.% LSA in 12:1 PEO-LiTFSI complex and the same amount of OEG in the same PEO-LiTFSI system. We can see in Fig. 5 that LSA-12a displayed a T_g of − 33.6 °C, while OEG-12a showed the transition at − 31.7 °C. LSA-12a caused a slightly lowering of glass transition temperature, meaning the crystallinity of polymer matrix can be further reduced by LSA, due to the asymmetric molecular structure with terminal OEG groups.

Electrochemical and thermal stability studies

Electrochemical studies of NOE and LSA

High electrochemical stability of polymer electrolytes is critical, and it is characterized by the cyclic voltammetry (CV)

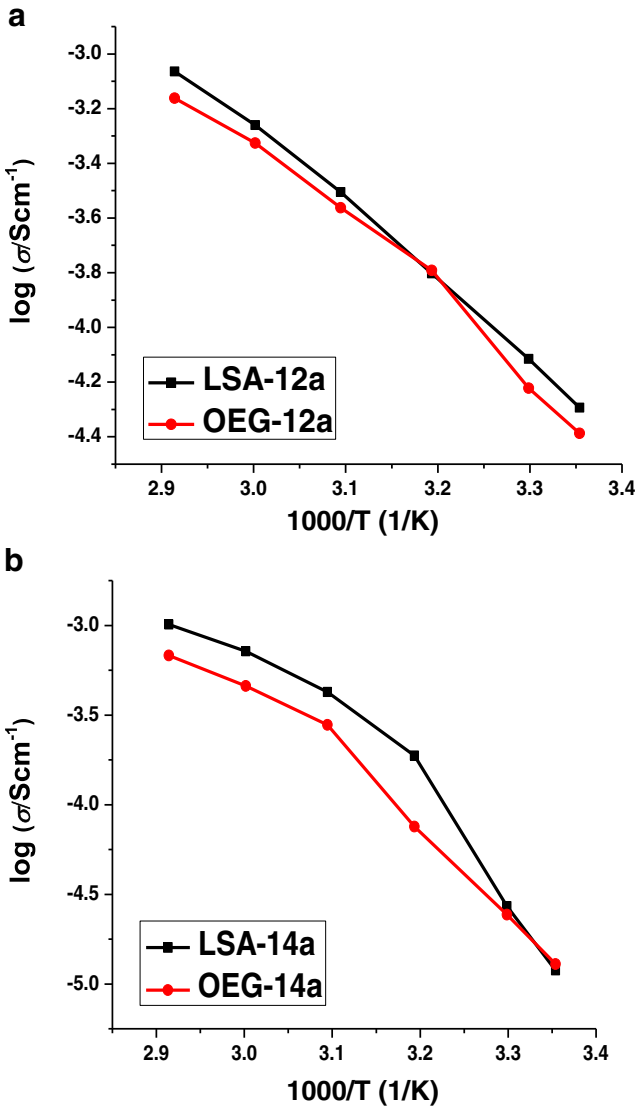

Fig. 3 Ionic conductivity versus temperature of LSA plasticizer compared with OEG in different PEO-LiTFSI complexes. Comparisons of 10 wt.% of LSA and OEG in 12/1 PEO-LiTFSI complexes (**a**); 10 wt% of LSA and OEG in 14/1 PEO-LiTFSI complexes (**b**)

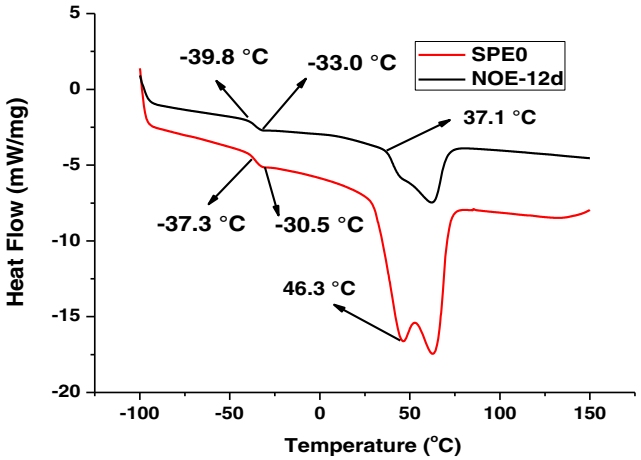

Fig. 4 DSC curves of SPE0 (red) and DOE-12d (black)

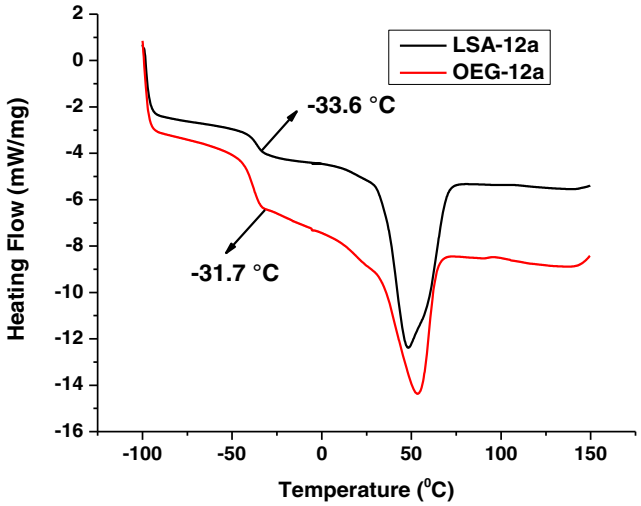

Fig. 5 DSC traces of LSA-12a (black) and OEG-12a (red)

experiment. NOE-12d was selected for further studies, because of its superior ionic conductivity. As can be seen in Fig. 6a, the oxidation peak of NOE-12d appeared at 4.2 V vs. Li/Li^+, compared with SPE0 (the reference) at 4.7 V vs. Li/Li^+. Though the electrochemical stability was dropped slightly after the addition of NOE, the resulting SPE is still

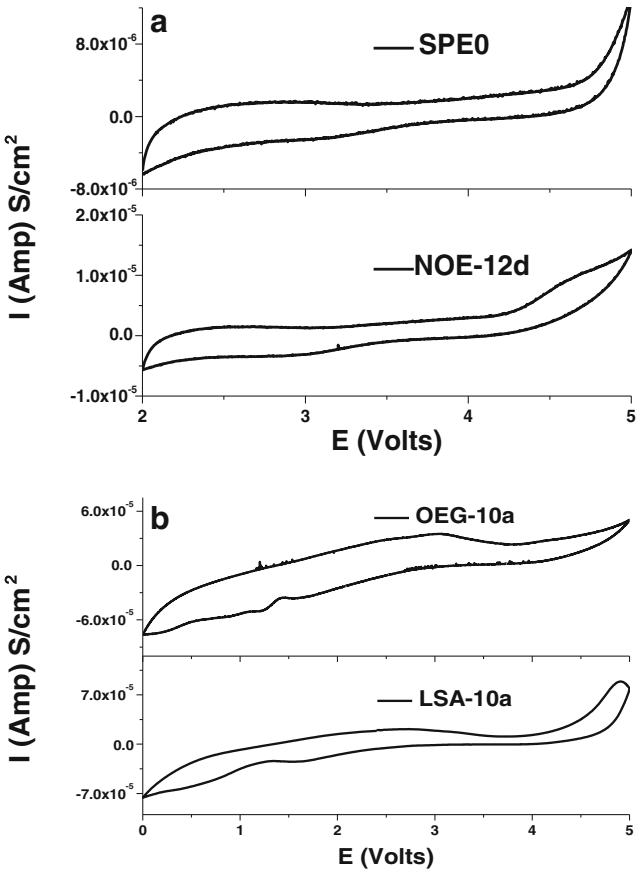

Fig. 6 Cyclic voltammograms of SPE0 (above) and NOE-12d (below) (**a**), OEG-101SPE1 (above) and LSA-101SPE1 (below) (**b**)

good to meet the electrochemical stability requirements for practical lithium polymer cells [50].

LSA-10a and OEG-10a were selected to perform electrochemical stability test by the method described above for a comparative study. The only difference was that the potential was anodically scanned from 0 to maximum 5.0 V versus Li^+/Li at a scan rate of 10 mV/s. As shown in Fig. 6b, LSA-10a exhibited electrochemical stability up to 4.2 V vs. Li^+/Li, which was similar to the OEG-plasticized SPE. Both NOE and LSA meet the minimum requirements of electrochemical stability for SPEs in LIBs (Table 6) [51].

Thermal stability studies of NOE and LSA

The thermal decomposition of SPE films was measured by the TGA. The high thermal stability of polymer electrolytes is preferred due to safety of Li-ion batteries. The samples were first heated to 110 °C to remove any moistures or any residual solvent molecules, then cooled to room temperature and re-heated up to 550 °C to measure the thermal stability. The result of the TGA experiment is depicted in Fig. 7a. It should be noted that NOE-12d starts to lose weight at around 250 °C and major loss of weight occurs after 350 °C. By contrast, the film without the additive showed excellent thermal stability up to 350 °C. Therefore, the pyrolysis temperature of the additive is in the range between 250 and 350 °C. The decomposition after 350 °C is primarily due to the degradation of C–O–C bonds of the host polymer [52]. The thermal degradation profile of LSA-10a and OEG-10a has also been evaluated. Figure 7b demonstrates that LSA-10a starts to lose weight at 350 °C and the film with OEG additive showed the decomposition temperature at slightly over 350 °C. This thermal stability trend is in well agreement with other similar work [53]. In general, the thermal stability and electrochemical stability of plasticizers are slightly inferior to PEO, because of their low molecular weight. Compare the work in this paper with borate ester plasticizer in previous published paper by our group [36]. The decomposition temperature is quite consistent for each sample and performs higher temperature than minimum requirements listed in Table 6. Thus, it can be concluded that the PEO-based SPEs containing both NOE and LSA plasticizer possess excellent thermal stability.

Table 6 Electrochemical and thermal stability minimum requirements for solid polymer electrolytes for LIBs

Parameter	Requirement
Stable potential window	≥ 4.0 V vs. Li^+/Li
Thermal stability	> 150 °C

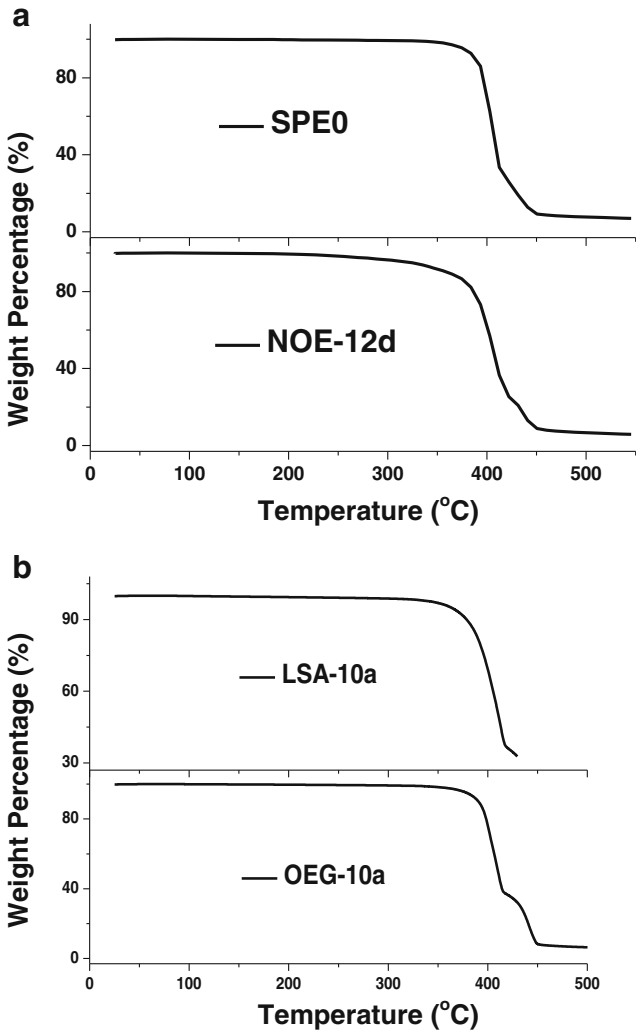

Fig. 7 TGA thermograms of SPE0 (above) and NOE-12d (below) (**a**); LSA-101SPE1 (above) and OEG-101SPE1 (below) (**b**)

Conclusions

In this study, two types of plasticizers (NOE and LSA) were designed, synthesized, and characterized as additives for PEO-based SPEs. Both plasticizers contain oligoether moiety to improve the compatibility with the PEO host. The effect of plasticizer content and lithium salt concentration on the properties of SPEs has been studied and discussed. Forty weight percent NOE in 12:1 PEO-LiTFSI complex displayed ionic conductivity of 1.11×10^{-4} S cm^{-1} at 313 K. Ten weight percent of LSA in 12:1 PEO-LiTFSI complex represented the best ionic conductivity of 5.08×10^{-5} S cm^{-1} at room temperature, and 10 wt.% LSA in 14:1 PEO-LiTFSI complex showed the best ionic conductivity of 1.88×10^{-4} S cm^{-1} at 313 K and 1.01×10^{-3} S cm^{-1} at 343 K. According to our study, LSA can further reduce the crystalline phases of PEO matrix compared to a standard oligoether compound. The effect of adding LSA or NOE plasticizer seems to slightly

reduce the thermal stability and electrochemical stability of the SPEs, but they still satisfy the minimum requirements of LIBs. In general, most PEO-based SPEs displayed good thermal stability and electrochemical stability. Ionic conductivity is the only parameter needed to be improved. In this work, we have developed SPEs with significantly improved ionic conductivity.

References

1. Nair JR, Porcarelli L, Bella F, Gerbaldi C (2015) Newly elaborated multipurpose polymer electrolyte encompassing RTILs for smart energy-efficient devices. ACS Appl Mater Interfaces 7:12961–12971. https://doi.org/10.1021/acsami.5b02729
2. Jo G, Jeon H, Park MJ (2015) Synthesis of polymer electrolytes based on poly(ethylene oxide) and an anion-stabilizing hard polymer for enhancing conductivity and cation transport. ACS Macro Lett 4:225–230. https://doi.org/10.1021/mz500717j
3. Rolland J, Brassinne J, Bourgeois JP et al (2014) Chemically anchored liquid-PEO based block copolymer electrolytes for solid-state lithium-ion batteries. J Mater Chem A 2:11839–11846. https://doi.org/10.1039/c4ta02327g
4. Gerbaldi C, Nair JR, Kulandainathan MA et al (2014) Innovative high performing metal organic framework (MOF)-laden nanocomposite polymer electrolytes for all-solid-state lithium batteries. J Mater Chem A 2:9948–9954. https://doi.org/10.1039/C4TA01856G
5. Wetjen M, Kim GT, Joost M et al (2014) Thermal and electrochemical properties of PEO-LiTFSI-Pyr 14TFSI-based composite cathodes, incorporating 4 V-class cathode active materials. J Power Sources 246:846–857. https://doi.org/10.1016/j.jpowsour.2013.08.037
6. Zhang J, Zhao J, Yue L et al (2015) Safety-reinforced poly(propylene carbonate)-based all-solid-state polymer electrolyte for ambient-temperature solid polymer lithium batteries. Adv Energy Mater 5:1–10. https://doi.org/10.1002/aenm.201501082
7. Colò F, Bella F, Nair JR et al (2015) Cellulose-based novel hybrid polymer electrolytes for green and efficient Na-ion batteries. Electrochim Acta 174:185–190. https://doi.org/10.1016/j.electacta.2015.05.178
8. Wei Z, Chen S, Wang J et al (2018) A large-size, bipolar-stacked and high-safety solid-state lithium battery with integrated electrolyte and cathode. J Power Sources 394:57–66. https://doi.org/10.1016/j.jpowsour.2018.05.044
9. Tominaga Y, Yamazaki K (2014) Fast Li-ion conduction in poly(ethylene carbonate)-based electrolytes and composites filled with TiO_2 nanoparticles. Chem Commun 50:4448–4450. https://doi.org/10.1039/c3cc49588d
10. Huang K-C, Li H-H, Fan H-H et al (2017) An *in situ*-fabricated composite polymer electrolyte containing large-anion lithium salt for all-solid-state $LiFePO_4$/Li batteries. ChemElectroChem 4:2293–2299. https://doi.org/10.1002/celc.201700322
11. Li YH, Wu XL, Kim JH et al (2013) A novel polymer electrolyte with improved high-temperature tolerance up to 170 °C for high-temperature lithium-ion batteries. J Power Sources 244:234–239. https://doi.org/10.1016/j.jpowsour.2013.01.148
12. Xue Z, He D, Xie X (2015) Poly(ethylene oxide)-based electrolytes for lithium-ion batteries. J Mater Chem A 3:19218–19253. https://doi.org/10.1039/c5ta03471j
13. Golodnitsky D, Livshits E, Ulus A, Peled E (2002) Highly conductive, oriented polymer electrolytes for lithium batteries. Polym Adv Technol 13:683–689. https://doi.org/10.1002/pat.266
14. Gray FM, Connor JA (1997) Polymer Electrolytes. Royal Society of Chemistry, London
15. Gadjourova Z, Andreev YG, Tunstall DP, Bruce PG (2001) Ionic conductivity in crystalline polymer electrolytes. Nature 412:520–523. https://doi.org/10.1038/35087538
16. He W, Cui Z, Liu X et al (2017) Carbonate-linked poly(ethylene oxide) polymer electrolytes towards high performance solid state lithium batteries. Electrochim Acta 225:151–159. https://doi.org/10.1016/j.electacta.2016.12.113
17. Zhang J, Wen H, Yue L et al (2017) In situ formation of polysulfonamide supported poly(ethylene glycol) divinyl ether based polymer electrolyte toward monolithic sodium ion batteries. Small 13:1–10. https://doi.org/10.1002/smll.201601530
18. Cheng S, Smith DM, Li CY (2014) How does nanoscale crystalline structure affect ion transport in solid polymer electrolytes? Macromolecules 47:3978–3986. https://doi.org/10.1021/ma500734q
19. Zhang J, Ma C, Liu J et al (2016) Solid polymer electrolyte membranes based on organic/inorganic nanocomposites with star-shaped structure for high performance lithium ion battery. J Membr Sci 509:138–148. https://doi.org/10.1016/j.memsci.2016.02.049
20. Chai J, Liu Z, Ma J et al (2017) In situ generation of poly (vinylene carbonate) based solid electrolyte with interfacial stability for $LiCoO_2$ lithium batteries. Adv Sci 4:1–9. https://doi.org/10.1002/advs.201600377
21. Olgun U, Gülfen M (2014) Synthesis of fluorescence poly(phenylenethiazolo[5,4-d]thiazole) copolymer dye: spectroscopy, cyclic voltammetry and thermal analysis. Dyes Pigments 102:189–195. https://doi.org/10.1016/j.dyepig.2013.10.049
22. Jung G-Y, Choi JH, Lee JK (2015) Thermal behavior and ion conductivity of polyethylene oxide/polyhedral oligomeric silsesquioxane nanocomposite electrolytes. Adv Polym Technol 34. https://doi.org/10.1002/adv.21499
23. Liang X, Yang Y, Jin X et al (2015) The high performances of SiO_2/Al_2O_3-coated electrospun polyimide fibrous separator for lithium-ion battery. J Membr Sci 493:1–7. https://doi.org/10.1016/j.memsci.2015.06.016
24. Ni'Mah YL, Cheng MY, Cheng JH et al (2015) Solid-state polymer nanocomposite electrolyte of TiO_2/PEO/$NaClO_4$ for sodium ion batteries. J Power Sources 278:375–381. https://doi.org/10.1016/j.jpowsour.2014.11.047
25. Pitawala HMJC, Dissanayake MAKL, Seneviratne VA et al (2008) Effect of plasticizers (EC or PC) on the ionic conductivity and thermal properties of the $(PEO)_9LiTf$: Al_2O_3 nanocomposite polymer electrolyte system. J Solid State Electrochem 12:783–789. https://doi.org/10.1007/s10008-008-0505-7
26. Niedzicki L, Kasprzyk M, Kuziak K et al (2009) Modern generation of polymer electrolytes based on lithium conductive imidazole salts. J Power Sources 192:612–617. https://doi.org/10.1016/j.jpowsour.2009.03.050
27. Wang H, Im D, Lee DJ et al (2013) A composite polymer electrolyte protect layer between lithium and water stable ceramics for aqueous lithium-air batteries. J Electrochem Soc 160:A728–A733. https://doi.org/10.1149/2.020306jes
28. Li Y, Zhan H, Wu L et al (2006) Flame-retarding ability and electrochemical performance of PEO-based polymer electrolyte with middle MW cyclic phosphate. Solid State Ionics 177:1179–1183. https://doi.org/10.1016/j.ssi.2006.05.015
29. Das S, Ghosh A (2017) Charge carrier relaxation in different plasticized PEO/PVDF-HFP blend solid polymer electrolytes. J Phys Chem B 121:5422–5432. https://doi.org/10.1021/acs.jpcb.7b02277
30. Karmakar A, Ghosh A (2010) A comparison of ion transport in different polyethylene oxide–lithium salt composite electrolytes. J Appl Phys 107:104113. https://doi.org/10.1063/1.3428389

31. Molinari N, Mailoa JP, Kozinsky B (2018) Effect of salt concentration on ion clustering and transport in polymer solid electrolytes: a molecular dynamics study of PEO–LiTFSI. Chem Mater. https://doi.org/10.1021/acs.chemmater.8b01955
32. Das S, Ghosh A (2015) Effect of plasticizers on ionic conductivity and dielectric relaxation of PEO-$LiClO_4$ polymer electrolyte. Electrochim Acta 171:59–65. https://doi.org/10.1016/j.electacta.2015.04.178
33. Polu AR, Rhee H-W (2017) Ionic liquid doped PEO-based solid polymer electrolytes for lithium-ion polymer batteries. Int J Hydrog Energy 42:7212–7219. https://doi.org/10.1016/j.ijhydene.2016.04.160
34. Chaurasia SK, Shalu S, Gupta AK et al (2015) Role of ionic liquid [$BMIMPF_6$] in modifying the crystallization kinetics behavior of the polymer electrolyte PEO-$LiClO_4$. RSC Adv 5:8263–8277. https://doi.org/10.1039/C4RA12951B
35. Ramesh S, Liew C-W (2012) Tailor-made fumed silica-based nanocomposite polymer electrolytes consisting of BmImTFSI ionic liquid. Iran Polym J 21:273–281. https://doi.org/10.1007/s13726-012-0022-5
36. Chakrabarti A, Filler R, Mandal BK (2008) Borate ester plasticizer for PEO-based solid polymer electrolytes. J Solid State Electrochem 12:269–272. https://doi.org/10.1007/s10008-007-0388-z
37. Henderson WA (2007) Crystallization kinetics of glyme - LiX and PEO - LiX polymer electrolytes. Macromolecules 40:4963–4971. https://doi.org/10.1021/ma061866d
38. Bernhard R, Latini A, Panero S et al (2013) Poly(ethylenglycol)dimethylether-lithium bis(trifluoromethanesulfonyl) imide, PEG500DME-LiTFSI, as high viscosity electrolyte for lithium ion batteries. J Power Sources 226:329–333. https://doi.org/10.1016/j.jpowsour.2012.10.059
39. Pradhan DK, Choudhary RNP, Samantaray BK et al (2007) Effect of plasticizer on structural and electrical properties of nanocomposite solid polymer electrolytes. Int J Electrochem Sci 2:861–871. https://doi.org/10.1007/s11581-010-0491-5
40. Vignarooban K, Dissanayake MAKL, Albinsson I, Mellander B-E (2014) Effect of TiO_2 nano-filler and EC plasticizer on electrical and thermal properties of poly(ethylene oxide) (PEO) based solid polymer electrolytes. Solid State Ionics 266:25–28. https://doi.org/10.1016/j.ssi.2014.08.002
41. Zhao Y, Wu C, Peng G et al (2016) A new solid polymer electrolyte incorporating $Li_{10}GeP_2S_{12}$ into a polyethylene oxide matrix for all-solid-state lithium batteries. J Power Sources 301:47–53. https://doi.org/10.1016/j.jpowsour.2015.09.111
42. Klongkan S, Pumchusak J (2015) Effects of nano alumina and plasticizers on morphology, ionic conductivity, thermal and mechanical properties of PEO-LiCF3SO3 solid polymer electrolyte. Electrochim Acta 161:171–176. https://doi.org/10.1016/j.electacta.2015.02.074
43. Gitelman L, Israeli M, Averbuch A et al (2007) Modeling and simulation of Li-ion conduction in poly(ethylene oxide). J Comput Phys 227:1162–1175. https://doi.org/10.1016/j.jcp.2007.08.033
44. Zardalidis G, Ioannou E, Pispas S, Floudas G (2013) Relating structure, viscoelasticity, and local mobility to conductivity in PEO/LiTf electrolytes. Macromolecules 46:2705–2714. https://doi.org/10.1021/ma400266w
45. Stephan AM (2006) Review on gel polymer electrolytes for lithium batteries. Eur Polym J 42:21–42. https://doi.org/10.1016/j.eurpolymj.2005.09.017
46. Sharma P, Kanchan DK, Gondaliya N et al (2013) Conductivity relaxation in Ag+ ion conducting PEO–PMMA–PEG polymer blends. Ionics (Kiel) 19:301–307. https://doi.org/10.1007/s11581-012-0738-4
47. Sengwa RJ, Kaur K, Chaudhary R (2000) Dielectric properties of low molecular weight poly (ethylene glycol) s. Polym Int 49:599–608. https://doi.org/10.1002/1097-0126(200006)49:6<599::AID-PI425>3.0.CO;2-K
48. Sengwa RJ, Dhatarwal P, Choudhary S (2014) Role of preparation methods on the structural and dielectric properties of plasticized polymer blend electrolytes: correlation between ionic conductivity and dielectric parameters. Electrochim Acta 142:359–370. https://doi.org/10.1016/j.electacta.2014.07.120
49. Sengwa RJ, Dhatarwal P, Choudhary S (2015) Effects of plasticizer and nanofiller on the dielectric dispersion and relaxation behaviour of polymer blend based solid polymer electrolytes. Curr Appl Phys 15:135–143. https://doi.org/10.1016/j.cap.2014.12.003
50. Ali AMM, Subban RHY, Bahron H et al (2013) Investigation on modified natural rubber gel polymer electrolytes for lithium polymer battery. J Power Sources 244:636–640. https://doi.org/10.1016/j.jpowsour.2013.01.002
51. Yue L, Ma J, Zhang J et al (2016) All solid-state polymer electrolytes for high-performance lithium ion batteries. Energy Storage Mater 5:139–164. https://doi.org/10.1016/j.ensm.2016.07.003
52. Ueno M, Imanishi N, Hanai K et al (2011) Electrochemical properties of cross-linked polymer electrolyte by electron beam irradiation and application to lithium ion batteries. J Power Sources 196:4756–4761. https://doi.org/10.1016/j.jpowsour.2011.01.054
53. Elizabeth RN, Kalyanasundaram S, Saito Y, Stephan AM (2005) Compatibility and thermal stability studies on plasticized PVC/PMMA blend polymer electrolytes complexed with different lithium salts. Polímeros 15:46–52. https://doi.org/10.1590/S0104-14282005000100011